

Modeling the Dynamics of a Smart Dental Drill

Sheela Hanagal
shanagal@andrew.cmu.edu

Minji Kim
minjik2@andrew.cmu.edu

December 8, 2018

1 Abstract

In our paper, we aim to develop and prove the safety of a model for a smart dental drill used for dental implants. This extends already existing research done on oil drills into a new field. We do so by developing models of the dynamics of such a drill, building up from basic properties, in order to prove that certain control decisions can ensure that the drill never hits a sensitive part of the gums. First, we develop a simple downward motion model with forces, progress to a model that incorporates angular motion, add friction forces to the same model, and then finalize with a time-triggered model, all models included with proofs. After discussing our models and proofs, we go on to discuss future improvements that could be made.

2 Introduction

As modern health care improves and people live longer, the need for better dental care arises. One such part of dental care that has needed improvement is the implant procedure. Implants are used for the purposes of supporting existing teeth and replacing missing teeth. Drills used for this procedure have improved over time, but there is still a level of risk when performing the procedure, due to the existence of a neurovascular bundle that dentists want to avoid hitting when drilling down into the gum. The development of a smart drill has attempted to improve the way we can detect this neurovascular bundle, however we want to investigate how we can ensure safety from the information that the smart drill provides. We want to ensure that using this smart drill will allow us to perform the necessary procedure and drill deep enough without hitting this neurovascular bundle.

We were inspired by the research paper *Towards abimodal proximity sensor for in situ neurovascular bundle detection during dental implant surgery* to pursue this smart drill system.[5]. The drill mentioned in the paper is a dental drill that uses sensors to detect the neurovascular bundle present underneath teeth in order to not hit the bundle in question. This would allow dental implant surgery to be more precise, since there would be no uncertainty about the location of the bundle and dentists would then not need to worry about drilling too deeply for the surgery. For our system we assume that we are drilling into the gums for an implant surgery.

3 Related Work

The related work that we've seen so far deals with other drilling situations such as oil drills and proofs of these models. There are also parts of the literature discussing a dental drill model without actually creating a mathematical model itself. We plan to take these ideas and create an advancement in the realm of cyber-physical system research by pulling from the existing literature on both ends to fit a simplified mathematical model specifically for dental drills themselves.

The first work that we've read and considered is *Hybrid automata: an insight into the discrete abstraction of discontinuous systems*, which discusses a model for the torque of an oil drill with two degrees of freedom [1]. This paper discusses an oil drillstring, and goes into models of varying difficulty to model the dynamics of the system. We looked at the model of the torque with two degrees of freedom in particular since it is the

simplest model for drillstrings we have seen, and it gives a good explanation for the reasoning behind the dynamics. We used this model to model the angular velocity, Ω , required for our rate of penetration ODE.

Nonlinear motions of a flexible rotor with a drill bit: stick-slip and delay effects discusses a model for a drill-string considering the effects of friction, axial motion, and torque [6]. This paper contains a more involved model, but gives an idea of what we need to consider, when modeling a drill system. In order to fully realize the dynamics of the system, we must consider torque, friction, rate of penetration, and lateral motion.

Towards a bimodal proximity sensor for in situ neurovascular bundle detection during dental implant surgery is where we got the idea of a smart dental drill. This paper discusses in great detail how the smart drill would work, and what is the main reasoning behind the conception of such a drill. It discusses how the drill would use sensors to obtain information about the whereabouts of the neurovascular bundle, in order to help the drill stop before this spot [5].

Torsional Vibration Control and Cosserat Dynamics of a Drill-Rig Assembly is where we got our rate of penetration model from. This model relates the rate of penetration into the rock for an oil drill, and the bit angular velocity, and weight on the bit. The paper as a whole discusses the dynamics of an oil drill, some of which is too complex for the scope of our project. However, it did help us to relate the rate of penetration and torque, which helped us understand the dynamics of the system more [4].

Modelling and Analysis of Stick-slip Behaviour in a Drillstring under Dry Friction influenced our friction model. The paper discusses the concept of dry friction in an oil drillstring, which models stick-slip behavior of a drill. It gives a complex frictional model that corresponds with this behavior. We derived our frictional model from this by making the assumption that our drill does not have the same stick-slip behavior and therefore does not necessarily need the function for the frictional coefficient present in the model presented by the paper [2].

4 High-Level Approach

For our drilling model, we came up with four incremental models, each one becoming more complex and including more realistic elements. We control both the torque that we give to the rotary on the drill and the weight that we put downwards onto the drill. Each of the models are ensuring safety which includes checking that we have not hit the neurovascular bundle yet and that the drill by the end is moving slowly enough to come to a stop before hitting the bundle.

In the end we produced four models. First we are proving the basic downward movement model where we discount the angular motion of the drill but still consider friction. The second model takes the angular motion of the drill into account but discounts the effect of friction. The third model is a friction model that combines ideas from the first and the second model. However, in this model we are accounting for the effects of friction within the angular motion of the drill, which affects the downward motion of the drill as well. The previous two models are event-triggered models, which means we can assume that we have access to information about the drill's position and speed at all times. However, this is not a very realistic situation. In reality, we only have access to information about the drill's speed and whereabouts at certain moments in time. Thus, our final model is a time-triggered version of our third model. This means that we can no longer stop our drill at any point but only definitively change the weight of bit and the torque that we apply at set time intervals, which adds an extra layer of complexity when considering the safety of the model which we will discuss further later in this paper.

In order to help prove safety, we made simplifications to our model. First, we assumed that the drill rotary and the drill bit move together as a unit with the same angular velocity. We also assumed that we would at least have access to drill information at intervals of time T , which is safe to assume since a smart drill provides information about the drill's position relative to the neurovascular bundle as well as information about the motion of the drill bit itself. In order to prove the time-triggered model we also upper-bounded the amount of distance that the drill bit would move downwards for the sake of a less complex proof. This is valid since we created an upper bound which will still prove the safety of the drill's motion if not guarantee the total efficiency of the drill's movement.

In addition, throughout the models we will be using variables within the models. Table 1 describes all of the variables that we will be using.

All Variables Used in Our Models	
Variable Name	Descriptions
Jr	drill's moment of inertia
rob	radius of bit
wob	weight on bit
sfriiction	static friction constant
kfriction	kinetic friction constant
d	neurovascular bundle location
T	max time interval
Ω	angular velocity of drill motor and bit
a1	relationship of wob to rop
a2	relationship of angular velocity to rop
c	constant for all opposing torques
u	Torque applied to drill bit
posFinal	position of drill after time T
	angular velocity after time T

Table 1: All variables used

5 Proof Techniques

Before we dive into the various models and their proofs, let us describe the various proof techniques we used when trying to prove essential concepts within our model.

One essential concept before we continue is the idea of loop induction. We use this when a part of our model can repeat over and over again. This is a condition that we know to be true when we begin the loop, from one iteration of the loop to another, and at the conclusion of our loop. We typically wrap our model with a loop since it is allowed to execute any number of times. Thus, loop induction is a vital tool since it allows us to make certain assumptions when considering one run of the ordinary differential equation (ODE) to the next run of the ODE [3].

In KeYmaera X, we can use the technique ODE if the equation that we're trying to prove has a closed form solution. Thus, when we talk about the proof method ODE this typically means that we can find a closed form solution, the preconditions themselves are false, or that there is an obvious way to make the conclusions based on the evolution domain constraint and the preconditions. The evolution domain constraint (usually denoted by Q) is the condition within our ODE that limits when our ODE can run. So for example, in the ODE below our evolution domain constraint is $t \leq T$, which means that we cannot continue running the ODE when $t > T$ [3].

$$\{x' = 1, t' = 1 \& t \leq T\}$$

However, proofs become more complicated when we don't have a closed form solution for our ODE or we cannot write down a solution for our ODE in first-order real arithmetic. That's when the proof cannot be solved automatically and we must either use a differential invariant, a differential cut, or differential weakening [3].

Assume we have some kind of condition that represents our safe state. Differential invariants (dI) are meant to prove that if we begin in a safe state (where the condition is true) and we're trying to remain in the safe state that a run of the differential equation will still let us remain in the safe state. This would mean that every vector in the vector field of our differential equation must lead to a safe state if it begins in a safe state [3]. We can ensure this property if this lemma holds:

$$\text{dI} \frac{\vdash [x' := f(x)](e)' = 0}{e = 0 \vdash [x' = f(x)]e = 0}$$

Figure 1: dI Lemma

Differential Cut (dC) proves that a condition C is an invariant of the system and then restricts the domain of the differential equation when trying to prove the real condition (let's call it P) using that condition C. In other words, if C is true for every possible evolution following the ODE then we can include condition C as an evolution domain constraint in our ODE when trying to prove P [3]. This lemma expresses this idea:

$$\text{dC} \frac{\Gamma \vdash [x' = f(x) \& Q]C, \Delta \quad \Gamma \vdash [x' = f(x) \& (Q \wedge C)]P, \Delta}{\Gamma \vdash [x' = f(x) \& Q]P, \Delta}$$

Figure 2: dC Lemma

Differential weakening (dW) is a proof concept that uses the information gained from the evolution domain constraint to prove a condition. We know that the evolution domain constraint Q restricts the evolution of a set of values in a differential equation to stay within a set of states such that Q still holds at the end of the evolution. Then, if the constraint Q can prove the condition at the end (let's call it P) of the differential equation, then no matter how the system evolved under the differential equation, we can prove that P is true after the continuous evolution no matter what the differential equation does [3]. This idea is expressed in this lemma:

$$dW \frac{Q+P}{\Gamma+ [v=f(x) \& Q]P.A}$$

Figure 3: dW Lemma

6 Basic Movement Model

6.1 Explanation of Model

To start, we decided to model a simple system based off of only the downward motion of the drill, taking into account a variable force applied, and how that would affect movement. This is a more basic version of our main drill model, where we are only taking into account the presence of a force that we have control over, and an opposing frictional force. In this simplified version, we do not account for rotational motion and variable friction in order for us to first think about the simple motion of the system and get used to thinking about the forces acting on the system. We will incorporate rotational motion and variable friction into later, more complex models.

The safety property being proved by this model, and all subsequent models, is that the position of the drill never exceeds the position of the neurovascular bundle. The depth at which the neurovascular bundle exists just after is defined by a variable d .

We first included a variable force that relates to the weight on the drill bit. We have the condition that the force should always be positive, since it should be applying the force to the drill to make it move downwards:

$$force := *;?(force > 0);$$

Using this force and the constant opposing force, we calculated the acceleration, using Newton's Second Law. Since the opposing friction force would differ based on whether our drill was in motion versus if our drill was stopped and wanted to resume motion, we included a check for this case, in which if the drill is stopped, it must have enough force to overcome the static opposing friction force in order to resume motion. We also ensure that if we are at a point where we must brake at the max braking acceleration in order to not hit the neurovascular bundle at depth d , the max braking acceleration is chosen. The point at which we must brake at max braking acceleration is modeled as follows:

$$vel^2/(2 * B) = d - pos$$

The left-hand side calculates the distance traveled if we brake at max braking acceleration B from the current velocity, to a stop. If this distance equals the distance away from the bundle, which is $d - pos$, then we are at the point where we must brake at this acceleration to ensure safety. The differential equations to model the movement of the drill are thus:

$$\begin{aligned} &\{pos' = vel, vel' = acc \& vel^2/(2 * B) \leq d - pos \& vel \geq 0\} \\ &\quad ++ \\ &\{pos' = vel, vel' = acc \& vel^2/(2 * B) \geq d - pos \& vel \geq 0\} \end{aligned}$$

where pos is the position of the drill, vel is the velocity of the drill, and acc is the acceleration of the drill. We also have an event trigger, which is an indicator that restricts the evolution domain of the differential equation system based on a certain property assuming we have knowledge of the position and velocity at all times, since we make a starting assumption that the smart drill has access to position at any given time. We will later on prove a model that gets rid of this assumption, however for simplicity in our initial model, this assumption was made. The event trigger

$$vel^2/(2 * B) = d - pos$$

is the point at which we must apply the maximum braking acceleration in order to not go past depth d , which then ensures that we choose that braking acceleration on the next iteration of our model, and brake safely. Thus, we ensure that the case that the position is greater than depth d never occurs, and were able to prove this safety property using KeYmaera X.

6.2 Proof strategy

Since this model is not as complex we did not need any complex proof techniques such as differential invariants for the proof. This model mostly relied on the arithmetic and conditions we created when setting the acceleration in order to guarantee correctness. For example, for our acceleration we only set a positive acceleration if $\frac{vel^2}{2B} < d - pos$. The model can only go into the differential equation system with the evolution domain constraint $\frac{vel^2}{2B} \leq d - pos$ while the above case is true, and breaks immediately when the condition $\frac{vel^2}{2B} = d - pos$ becomes true. This is the point at which the amount of distance that would be traveled when braking at max acceleration is equal to the amount of distance at which we are away from the neurovascular bundle, represented by depth d . Then at that point, our model ensures that the acceleration can only be set to $-B$, thus ensuring that we will break in time such that $pos \leq d$ and $\frac{vel^2}{2B} \leq d - pos$ are both always true.

The differential equations proved with ODE after we broke down the accelerations into the possible cases (positive acceleration, some negative acceleration, or $-B$).

7 Angular Motion Model

7.1 Explanation of the Model

For this model as well, our goal for safety is the same as we discussed in the downward movement model. The position of the drill will still not hit the neurovascular bundle or $pos \leq d$. We also want to ensure that if the drill is still moving downwards that we can stop it in time before hitting the neurovascular bundle. This is represented by the equation

$$((a2 * Jr * \Omega)/c) \leq d - pos$$

which we will discuss further below. However, in this model we are considering the angular velocity of the drill and how that angular movement affects the downward movement of the drill. This is also still an event-triggered model. We are not considering the effects of friction in this model.

The model that we created to represent the drill's angular motion behavior was adapted from the model from the paper by Navarro-Lopez and Cortes [5]. The model from this paper is for a more complex drillstring system for oil and gas drilling. Our system is a simpler version of this system, so we adopted the 2-DOF model that was presented in the paper. The original model they had was:

$$\begin{aligned} x_1' &= \frac{1}{J_r} [-(c_t + c_r)x_1 - k_t * x_2 + c_t * x_3 + u] \\ x_2' &= x_1 - x_3 \\ x_3' &= \frac{1}{J_b} [c_t * x_1 + k_t * x_2 - (c_t + c_b) * x_3 - T_{f_b}(x_3)] \end{aligned}$$

First, to define all of the variables used, x_1 is the angular velocity of the rotary system of the drill, x_2 is the difference in the angular displacements of the rotary system and the drill bit, and x_3 is the angular velocity of the drill bit. J_r is the rotational inertia of the rotary system, while J_b is the rotational inertia of the drill bit. c_t is the torsional damping of the drill pipe, and the k_t is the torsional stiffness of the drill pipe, which is being represented by a spring. $c_r * x_1$ is the damping torque at the rotary system, u is the torque applied by the motor, and $T_b = c_b * x_3 + T_{f_b}$ is the torque on the drill bit, where $T_{f_b} = f_b * \text{sign}(x_3)$ models the frictional contact with bit rock where $f_b = W_{ob}R_b[u_{cb} + (u_{sb} - u_{cb})\exp(-y_b/v_p|x_3|)]$. W_{ob} is the weight on the drill, R_b is the bit radius, u_{sb} is the static friction coefficient, while u_{cb} is the Coulomb friction coefficient, both associated with J_b .

Now in our model, we assumed that the drill bit and the drill rotary are one connected component. In other words, we assumed that they move with the same angular velocity and change angular velocity due to the same torque. This makes $x_2 = 0$ and we combine ideas from x_1 and x_3 in order to represent the total angular velocity of the drill components. The equation that we came up with is a much more simplified version which is

$$\Omega' = \frac{1}{Jr} * (-c * \Omega + u)$$

where

$$\Omega$$

is the angular velocity of the drill components and thus

$$\Omega'$$

is the change in that angular velocity. The opposing forces that come from the damping torque of the rotary system is represented by c . We do not need to consider the torsional damping from the drill pipe since we are considering the drill rotary and the bit as one connected component. Then, u is the torque that is being applied, which the operator of the drill can control. We allow this value to be set to any positive value. We ignore friction in this model.

Then, according to Tucker and Wang's paper we got an equation for the rate of penetration. They represented rate of penetration with the equation

$$ROP = -a1 + a2 * WOB + a3 * \Omega$$

We ignore the constant $a1$ in our model since we never want to allow the rate of penetration to be negative. ROP is the rate of penetration, WOB is the weight on the bit, Ω is the angular velocity of the drill, $a1$ and $a2$ are constants that relate WOB and Ω respectively to the rate of penetration [4]. These were measured to be integer constants in the oil drill model but we will leave them as variables for now since we do not know the precise values of $a1$ and $a2$ for a dental drill. This model also relates the angular velocity of the drill to the downward movement of the drill, which is exactly what we wanted. Thus, our resulting model for the downward movement of the drill is

$$pos' = a1 * wob + a2 * \Omega$$

where pos is the position of the drill, pos' is the rate of penetration. Much like u we also allow WOB to be changed to any value by the user of the drill. Thus, before we run our ODEs containing pos' and Ω' we set the torque and the weight on the bit as such

$$wob := *;?(wob > 0 \& ((a2 * Jr * \Omega)/c) < d - pos); wob := 0;$$

$$u := *;?(u > 0 \& ((a2 * Jr * \Omega)/c) < d - pos); u := 0;$$

Essentially we ensure that both of the values are greater or equal to 0. Also, in order to set u and wob to any other value besides 0 we must also make sure that it is safe to continue motion without turning off the motor and releasing pressure from the bit.

Recall that the only values that the user can control are u and wob . The issue is that even if we set both wob and u to be 0, the drill is still moving downwards due to the $a2 * \Omega$ in the pos' term. Thus, we need $\Omega = 0$ if the drill is to stop moving downwards. Now when $((a2 * Jr * \Omega)/c) = d - pos$, this is the critical point where if we stop increasing Ω 's value it will eventually decay to 0 right as we arrive at the position d due to the term $-c * \Omega$ in the equation for Ω' . However, if we don't stop increasing Ω at this point we will go past d . This is also why we must make the safety check that $((a2 * Jr * \Omega)/c) < d - pos$ before we set wob and u to any value that is not 0.

Since this is also the critical point at which wob and u must become 0, this is also the event-trigger for our ODE. Our drill can only continue moving downward with non-zero wob and u values as long as $((a2 * Jr * \Omega)/c) \leq d$. This leads us to describe the drill's overall downward motion in this model with the ODEs:

$$\{pos' = a1 * wob + a2 * \Omega, \Omega' = \frac{1}{Jr} * (-c * \Omega + u) \& \Omega \geq 0 \& ((\frac{a2 * Jr * \Omega}{c}) \leq d - pos)\}$$

++

$$\{pos' = a1 * wob + a2 * \Omega, \Omega' = \frac{1}{Jr} * (-c * \Omega + u) \& \Omega \geq 0 \& ((\frac{a2 * Jr * \Omega}{c}) \geq d - pos)\}$$

Much like the previous model, the second differential equation allows for all possible real-life scenarios where $((\frac{a2 * Jr * \Omega}{c}) \leq d - pos) \geq 0$ and $((\frac{a2 * Jr * \Omega}{c}) \leq d - pos) \leq 0$

7.2 Proof Strategy

In order to prove the associated model, let's first discuss how we got the inequality

$$((\frac{a2 * Jr * \Omega}{c}) \leq d - pos)$$

So first let's consider Ω' or the differential equation describing how the angular velocity of the drill bit changes.

$$\Omega' = \frac{1}{Jr} * (-c * \Omega + u)$$

but we can take away the u term since we can set it to be a minimum value of 0, which we do if we want Ω to begin decreasing as we are approaching the neurovascular bundle. The closed form solution of the equation $\Omega' = \frac{1}{Jr} * (-c * \Omega)$ is then

$$\Omega(t) = \Omega_0 e^{\frac{-c * t}{Jr}}$$

This represents the value of Ω at any time t where Ω_0 is the initial value of Ω right when we set wob and u to be 0. We can plug this value of Ω back into the pos' equation to represent at each point in time what the change in position will be. Recalling that $wob = 0$, we then get the equation

$$pos' = a2 * \Omega(t)$$

In order to determine the total change in position we then integrate this in relation to t from 0 to . This give us a total change of position. When integrating $\Omega_0 e^{\frac{-c * t}{Jr}}$ from 0 to we get $\frac{Jr * \Omega}{c}$, which we must still multiply by $a2$ according to our position integral. Thus, the total change in position with the decaying value of Ω is $\frac{a2 * Jr * \Omega}{c}$. Thus, all of our safety checks that this total change in position is still less than or equal to the total amount of distance between the neurovascular bundle and the current position of the drill. Thus, our safety check includes the check that

$$((\frac{a2 * Jr * \Omega}{c}) \leq d - pos)$$

Now, let's consider the proof for our model. When proving this model we must consider multiple cases. These cases arise because $wob = 0$ or $wob = *$, $u = 0$ or $u = *$, and we can use either of the ODEs specified.

Since this model is event triggered most of our cases proved rather easily. Recall that our ending safety condition is

$$pos \leq d \& ((\frac{a2 * Jr * \Omega}{c}) \leq d - pos)$$

We can ensure this condition holds for our model that contains

$$((\frac{a2 * Jr * \Omega}{c}) \leq d - pos)$$

in its evolution domain constraint. This is because if its in the evolution domain constraint we know by differential weakening that it must also be true at the end of the evolution of the differential equation. Since most of these values are guaranteed to be positive constants and we also have an evolution domain constraint that $\Omega \geq 0$, we can guarantee that $a2, Jr, \Omega, c$ are all positive this also implies that $pos \leq d$.

The hard part of the proof is when

$$((\frac{a2 * Jr * \Omega}{c}) \geq d - pos)$$

. We know by the check that we performed after setting wob and u , that these two values must now both be 0. All other possible cases where $wob \neq 0$ or $u \neq 0$ are not considered since these cases are not even possible. Now, the only case in which our safety condition still holds is when

$$(((\frac{a2 * Jr * \Omega}{c}) = d - pos)$$

. Thus, we must make a differential cut with this condition. This differential cut proves by differential invariant, and then we can prove

$$\left(\left(\frac{a2 * Jr * \Omega}{c}\right)\right) \leq d - pos$$

with

$$\left(\left(\frac{a2 * Jr * \Omega}{c}\right)\right) = d - pos$$

quite trivially.

We can prove the differential invariant because the preconditions and the loop invariant guarantees that at the beginning of each each iteration of the ODE

$$\left(\left(\frac{a2 * Jr * \Omega}{c}\right)\right) = d - pos$$

was true. Thus, in order to be in this case we know that

$$\left(\left(\frac{a2 * Jr * \Omega}{c}\right)\right) = d - pos$$

must be true.

8 Friction Model

8.1 Explanation of Model

This is another event-triggered model which proves that the drill will not hit the neurovascular bundle in its movement.

This model is a combination of ideas from the previous model and the very first model that we have discussed. It takes the model from before that takes into consideration the angular movement of the drill into the downward movement of the drill. However, it also considers friction and its effect on the angular movement of the drill and thus the overall movement of the drill. In order to introduce this concept we introduce two new constants *sfriiction* and *kfriction*. This represents the coefficients of static friction and kinetic friction respectively and helps determine the overall value of friction. Recall this equation

$$T_{f_b} = f_b * sign(x_3), f_b = W_{ob}R_b[u_{cb} + (u_{sb} - u_{cb})exp(-y_b/v_p|x_3|)]$$

from the paper by Navarro-Lopez and Cortes [5]. We use these to approximate the effect of friction on the angular motion of the drill. Remember that we have simplified our model to consider angular velocity of the entire drill rather than the individual components so we can replace x_3 with Ω . Well we can ignore $sign(x_3)$ since we know that Ω is always greater or equal to 0 in our case. Then we simplify $[u_{cb} + (u_{sb} - u_{cb})exp(-y_b/v_p|x_3|)]$ to be either the constant *sfriiction* or *kfriction*. This is because after reading the paper by Navarro and Suarez, the friction model above was derived due to the stick-slip motion nature of an oil drill. We can make the assumption that the dental drill does not follow this motion. This is to simplify the math, and also because we do not believe that this same nature is held for a dental drill. We also assume for simplification of our model's proof that friction has no other effect on the movement of the drill.

The biggest consideration that we needed to make was whether to use static friction or the kinetic friction coefficient. Static friction is what our drill must overcome when it is not already in motion and kinetic friction is in effect when the drill is in motion. Thus, we used the kinetic friction coefficient any time that $\Omega > 0$, and considered static friction anytime $\Omega = 0$. The force that counteracts friction is the torque that we apply in our model. Thus, this is what our assignment of friction looked like:

$$?(\Omega > 0 | u > sfriiction * wob * rob); friction := kfriction * wob * rob;$$

++

$$?(\Omega = 0 \& u \leq sfriiction * wob * rob); friction := u;$$

Essentially like I just mentioned, if $\Omega > 0$, then we can use $kfriction$ as our coefficient for friction and calculate our total effect of friction as $kfriction * wob * rob$. Then, when $\Omega = 0$ we compare the torque to the effect of friction using the static friction coefficient. If $u > sfriction * wob * rob$, then we overcome static friction and begin to move, which means that we must use kinetic friction to represent kinetic friction. Otherwise, if $u < sfriction * wob * rob$, then the model must not be moving since it cannot overcome friction. Thus friction is applying as much force to exactly counteract the torque and our friction is set to u .

The other aspects of this friction model are exactly the same as the angular motion model, so I will not discuss the model again here.

8.2 Proof Strategy

The main safety condition,

$$\left(\frac{(a2 * Jr * \Omega)}{c}\right) \leq d - pos$$

does not change from the previous model when we include friction for this model. This is because when we mean to stop the drill completely we make both wob and u equal to 0 as we mentioned before. Our assigned friction is either equal to $kfriction * wob * rob$ or u which both evaluate to 0, when stopping the drill.

Since we did not significantly change our model, our proof for this model was also much the same. There were more cases that we had to consider simply because there are different possible values when we assign friction. However, the cases where

$$\left(\frac{(a2 * Jr * \Omega)}{c}\right) \leq d - pos$$

in the evolution domain constraint still prove the safety condition easily since we cannot escape our evolution domain during any run of our ODE.

We still must consider the case when

$$\left(\frac{(a2 * Jr * \Omega)}{c}\right) \leq d - pos$$

is in the evolution domain constraint instead. In this case, like discussed in the previous model, we do not consider any cases where wob or u are not 0 since the check when setting wob and u to any arbitrary value does not allow for this case. Friction however does not have any effect in these cases as mentioned before though. Thus, we can make a differential cut with

$$\left(\frac{(a2 * Jr * \Omega)}{c}\right) = d - pos$$

as before. We then prove that this cut is valid using differential invariant and prove the postcondition is true with differential weakening as we did in the previous model.

9 Time-Triggered Model

9.1 Explanation of Model

The time-triggered model ensures a more realistic scenario than our previous models, where we assume that we do not have access to the position and angular velocity of the drill at all times. The assumption made is that we have access at least every T seconds, which is a fair assumption to make since sensors are being used to detect these values in the smart drill.

Similar to the friction model discussed previously, downward movement is modeled by the same rate of penetration differential equation, angular motion is modeled by the same differential equation, and friction is modeled by the same equation. The difference now is that we cannot do the same analysis as before where we set the weight on bit to zero and turn off the motor and thus have the torque represented by u be zero as soon as we reach the point where we can bound the position change to stop right at depth d , as in the

previous model. Due to the fact that we do not have access to position and angular velocity at all times, more estimations and calculations need to be made. Other than this assumption, every other assumption made for the previous model remains the same.

In this model, same as before, we set the weight on bit and torque to be any value, unless we are at the point where we must set both to zero in order to stop in time before depth d , which was calculated as in the previous model by $\frac{(a2 * \Omega * Jr)}{c}$, giving us, as one example:

$$wob := *; ?(wob > 0((\frac{a2 * Jr * \Omega}{c}) < d - pos); ++ wob := 0;$$

Then we set our frictional force based on whether the drill is in motion, or at rest, just as in the previous model.

Next, we must check whether based on the weight on bit, torque, and frictional force that were set, after moving based on the differential equations (same as before) for time T , our drill would still be able to stop before the neurovascular bundle. Solving the differential equations for the actual equations for pos and Ω led to complex equations that included exponential terms. In order to simplify the calculations, we instead used upper bounds on these equations for our calculations.

An upper bound on $\Omega' = \frac{1}{Jr}(-c * \Omega + u - friction)$ is $\Omega' \leq \frac{1}{Jr}(u - friction)$, since we have already set Ω to be greater than or equal to zero, and $-c < 0$. Thus, solving for Ω gives us the upper bound on Ω :

$$\Omega \leq \Omega_0 + \frac{1}{Jr}(u - friction) * t$$

Since pos' includes Ω within it, we can substitute in to get $pos' \leq a1 * wob + a2 * (\frac{1}{Jr}(u - friction) * t + \Omega_0)$. Differentiating this gives us an upper bound on pos :

$$pos \leq pos_0 + a1 * wob * t + a2 * (\frac{1}{Jr} \frac{(u - friction) * t^2}{2} + \Omega_0 * t)$$

Thus, the Ω equation, when substituting for T , gives us the upper bound on the angular velocity at the end of time T , and the position equation gives an upper bound on the position of the drill after time T . Better upper bounds can be obtained with more rigorous mathematical techniques, however those bounds are not within the scope of what we can achieve at this time. We can use this knowledge to then check whether our drill would be able to stop before depth d after time T . We already have the property from the previous model that $\frac{(a2 * \Omega * Jr)}{c}$ is the bound for the position change after both the weight on bit and torque from the motor are zero. We can use this equation and our upper bounds to calculate whether the drill is safe after time T , by substituting T into the upper bounds and substituting them into our check $\frac{(a2 * \Omega * Jr)}{c} \leq d - pos$, giving us:

$$\begin{aligned} & \frac{(a2 * \Omega_0 + \frac{1}{Jr}(u - friction) * t * Jr)}{c} \\ & \leq \\ & d - (pos_0 + a1 * wob * t + a2 * (\frac{1}{Jr} \frac{(u - friction) * t^2}{2} + \Omega_0 * t)) \end{aligned}$$

Thus, using this, if the drill is safe after time T , we can allow the drill to follow the differential equations, and the same applies for each loop iteration. The differential equations for this model are very similar to the previous models, except we do not have two cases and an event trigger anymore, but instead have a domain constraint based on time t :

$$\begin{aligned} pos' &= a1 * wob + a2 * \Omega, \\ \Omega' &= (1/Jr) * (-c * \Omega + u - friction), \\ t' &= 1 \&\Omega >= 0 \&t <= T \&t >= 0 \end{aligned}$$

In the end, we would like to prove that no matter when we stop, $pos \leq d$ is true.

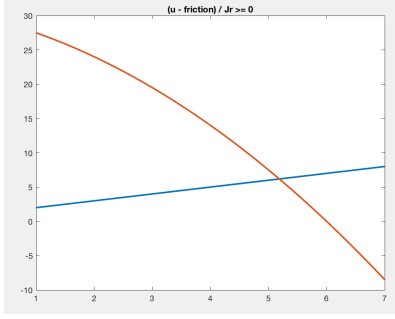


Figure 4: $(u - friction)/Jr \geq 0$

9.2 Proof Strategy

The goal is to prove that if we start off in a situation where we have enough distance to stop before the neurovascular bundle, then we never go beyond the neurovascular bundle. In our model, we already included the check that the drill initially starts this way, and after time T would remain this way as well. Thus, we need to prove that this holds in between at times $0 \leq t \leq T$ as well.

Since we used upper bounds on both Ω and pos when calculating the check on whether the drill is safe after time T , we must utilize differential cuts when proving the model in order to be able to use this information about these upper bounds when proving the model. Thus, differential cuts inserting $\Omega \leq \Omega_0 + \frac{1}{J_r}(u - friction) * t$ and $pos \leq pos_0 + a1 * wob * t + a2 * (\frac{1}{J_r} \frac{(u - friction) * t^2}{2} + \Omega_0 * t)$ were used. The cut changed based on the different cases present in the proof, such as the use of static friction instead of kinetic friction, or cases where the motor was turned off, the weight on bit was zero, or any combination thereof, with the proper terms being substituted into the equations above as a result.

The differential invariant technique was used to prove that these upper bounds hold for any times $0 \leq t \leq T$, which involves taking the derivative of these bounds, and proving the result using the differential equations and domain constraints. To use this information to prove the loop invariant that after any time $0 \leq t \leq T$, the drill is still safe and can be brought to a stop before depth d , the differential weakening technique must be used, along with quantifier elimination. This technique uses the information present about constants and the domain constraints to prove the resulting property with arithmetic.

A change in the model that resulted due to a difficulty in proving the model described was casing on whether $(u - friction)/Jr$ is negative or non-negative. The reasoning behind this change was because the pos upper bound is quadratic, and the Ω upper bound is linear, despite the fact that we check whether after time T , $\frac{(a2 * \Omega * Jr)}{c} \leq d - pos$, the left-hand side may not be less than the right-hand side for all times in between 0 and T with the current information and bounds we have. It could be that the line for the left-hand side intersects the quadratic form of the right-hand side at some point in $0 \leq t \leq T$, causing the inequality to hold at time T , but not some time in between.

This cannot be the case for when $(u - friction)/Jr \geq 0$, where the resulting quadratic is then as shown in Figure 4. This is because if the red line representing the left-hand side starts below the quadratic line, if it is below the quadratic line at time T , it must not have crossed in between.

However, the same does not apply for when $(u - friction)/Jr < 0$, which could result in a case as in Figure 5, where it initially and finally is below the quadratic line, but crossed above in between. Thus, for the case where $(u - friction)/Jr < 0$, we use a weaker upper bound for pos , which is:

$$pos \leq pos_0 + a1 * wob * t + a2 * \Omega_0 * t$$

. If $(u - friction)/Jr < 0$, $a2 * \frac{1}{J_r} \frac{(u - friction) * t^2}{2}$ is negative anyway, which can only bring down the value, and thus the upper bound is valid.

Using this upper bound eliminates the case where the left-hand side could be less than the right-hand side of the inequality at any point in-between if the inequality holds at times 0 and T , as shown in Figure 6. Thus, adding this case to our model enabled us to prove the model. The original differential cut for pos

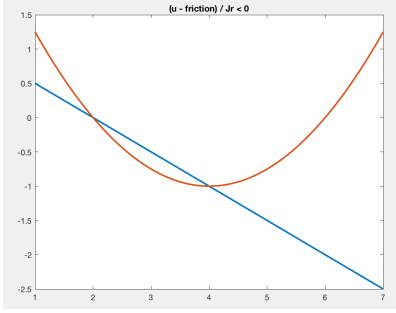


Figure 5: $(u - friction)/Jr < 0$

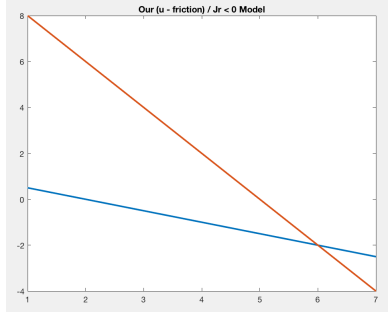


Figure 6: New Bound for $(u - friction)/Jr < 0$

was used for all cases where $(u - friction)/Jr \geq 0$, but a new differential cut using this new upper bound was used for all cases where $(u - friction)/Jr < 0$.

Thus, using all of these techniques, we were able to prove the safety property that $pos \leq d$, and if the drill were to continue onwards after the end of the model, $\frac{(a2 * \Omega * Jr)}{c} \leq d - pos$, so it can still safely stop.

10 Takeaways

Our project went differently from what we originally thought we would be able to achieve, with us simplifying the original model we took from the papers even more so than planned due to the mathematical complexity of the models. What we've learned is that modeling the exact dynamics of a system may end up more complex than expected, with the mathematics and intuition necessary for such models being more complex as a result. Therefore, we must always be prepared for simplifications. Additionally, even if a model may seem less complex, the proof may not be. Proving safety is a difficult, but worthwhile task.

11 Future Extensions

Due to the assumptions that we made, our current models do not fully cover the entire dynamics of a dental drill. Thus, if more research were to be done into the dynamics of the drill, several steps should be taken. To improve our own model, we would use the actual equations for pos and Ω , which included exponential terms, would make the model more precise. Re-incorporating the differences between the rotary motion and the drill motion is another step that should be taken, which would send the analysis of the model into more complex differential equation analysis. However, the reality of the system is such that there may be differences between the motions of the two parts, which should be accounted for in a full-fledged model. Having a more accurate friction model should also be a step. We extrapolated our friction model from an oil drillstring paper, however the actual dynamics of friction for a dental drill may not be exactly the same.

12 Deliverables

The deliverables are .kya and .kyx files containing our models of the smart drill completing the implant procedure and the proofs showing its safety.

13 Special Thanks

A special thanks to Professor Andre Platzer, and our TAs Yong Kiam Tan and Mengze Li for all of their feedback and help for our models and proofs! Thank you as well to Andrew Sogokon for pointing us in the right direction for drilling models. This project would not have been possible without their support.

14 Distribution of Work

Equal work was done by both members of the group.

References

- [1] Eva M. Navarro-López and Rebekah Carter. Hybrid automata: an insight into the discrete abstraction of discontinuous systems. *International Journal of Systems Science*, 42(11):1883–1898, November 2011.
- [2] Eva M. Navarro-López and R. Suarez. Modelling and analysis of stick-slip behaviour in a drillstring under dry friction. *Congreso de la AMCA*, pages 330–355, October 2004.
- [3] Andre Platzer. *Logical Foundations of Cyber-Physical Systems*. Springer International Publishing, Cham, Switzerland, 2018.
- [4] Robin W. Tucker and Charles Wang. Torsional vibration control and cosserat dynamics of a drill-rig assembly. *Meccanica*, 38:143–159, 2003.
- [5] Jessie R. Weber, Francois Baribeau, Paul Grenier, and et al. Towards a bimodal proximity sensor for in situ neurovascular bundle detection during dental implant surgery. *Biomedical Optics Express*, 5(1):16–30, December 2013.
- [6] Xinhua Long Guang Meng Xianbo Liu, Nicholas Vljajic and Balakumar Balachandran. Nonlinear motions of a flexible rotor with a drill bit: stick-slip and delay effects. *Nonlinear dynamics*, 72(1-2):61–77, April 2013.